Enhanced Aqueous Photochemical Reaction Rates after Freezing

Amanda M. Grannas,* Alexandra R. Bausch, and Kendell M. Mahanna

Department of Chemistry, Villanova University, 800 Lancaster Avenue, Villanova, Pennsylvania 19085

Received: May 16, 2007; In Final Form: August 6, 2007

Sunlit snow/ice is known to play an important role in the processing of atmospheric species, including photochemical production of NO_x, HONO, molecular halogens, alkyl halides, and carbonyl compounds, among others. It has been shown that a liquid-like (quasi-liquid or disordered) layer exists on the surface of pure ice and that this quasi-liquid layer is also found on the surface of ambient snow crystals and ice at temperatures similar to polar conditions. However, it is unclear what role the liquid-like fractions present in and on frozen water play in potential photochemical reactions, particularly with regard to organic substrates. Here, we report a detailed study of enhanced rates of photochemical nucleophilic substitution of *p*-nitroanisole (PNA) with pyridine, a well-characterized and commonly used actinometer system. Reaction rates were enhanced by a factor of up to ∼40 when frozen at temperatures between 236 and 272 K. Reaction rates were dependent on temperature and solute concentration, both variables that control the nature of the liquid-like fraction in frozen water. The results obtained indicate that a major portion of the organic solutes is excluded to the liquid-like layer, significantly impacting the rate of the photochemical nucleophilic substitution reaction studied here. Also, the direct comparison of liquid-phase kinetics to reactions occurring in frozen water systems is drawn into question, indicating that a simple extrapolation of liquid-phase mechanisms to snow/ice may not be valid for certain reactions.

Introduction

Heterogeneous chemistry plays an important role in a variety of atmospheric processes, including the recycling of reactive halogens critical to stratospheric ozone depletion, oxidation of SO_2 to sulfuric acid, and uptake of reactive gases on sea-salt aerosols, among others. Recent laboratory and field studies indicate that snow and ice play a crucial role in processing atmospheric species. The release of molecular halogens[1] from sunlit snowpacks can lead to the removal of ozone in the tropospheric marine boundary layer in Arctic regions during polar spring.[2] This ozone depletion chemistry is also linked to the transformation of elemental mercury to reactive gaseous and particle-phase mercury.[3] It has been shown that sunlit snow in both polar and mid-latitude regions can serve as a source of gas-phase NO_x and HONO via nitrate photolysis chemistry.[4] Detailed laboratory experiments have quantified NO_x production, studied quantum yields in frozen systems, and elucidated subsequent reactions of nitrogen oxides with organics present in snow.[5−7] Photochemical production of various organic compounds has been observed in snow and ice, including formaldehyde,[8] acetaldehyde and acetone,[9,10] alkyl halides,[11] and hydrocarbons.[12] Multiphase box models suggest that the measured fluxes of these compounds may have significant impacts on the overlying atmosphere.[13,14]

The chemistry that results in the production of such varied compounds, however, is not clearly understood. It has been shown that a liquid-like (quasi-liquid or disordered) layer exists on the surface of pure ice[15,16] and that this quasi-liquid layer is also found on the surface of ambient snow crystals and ice at temperatures relevant to polar conditions.[17] Many processes can take place when freezing a solution, including the formation of grain boundaries (the surface between two monocrystalline ice grains), veins (the linear intersections of grain boundaries), and nodes (the junction of veins). As ice forms from freezing water, pure water crystallizes first, and ions are excluded from the bulk and become concentrated at the surface.[18] Fast, nonequilibrium freezing will cause solutes to become trapped in micropockets of highly concentrated solution or incorporated into grain boundaries, veins, and nodes. These processes lead to a chemically enriched liquid-like layer at the surface, grain boundaries, and interstitial pores of snow and ice. Potential reactants could be highly concentrated (depending, in part, on their aqueous solubility), and the pH in these regions could be significantly different than what would be measured in a bulk sample. A number of descriptions have been used for these liquid-like areas, including the quasi-liquid layer (QLL), liquid-like layer (LLL), disordered layer, and so forth. It should be pointed out that this terminology has been used rather loosely in the literature, and it is still unclear whether solutes are incorporated into a true quasi-liquid layer or actual liquid water within the ice sample. An extensive discussion of the fundamental nature of snow and ice microphysics has recently been addressed in a review by Dominé et al.[19] As discussed there, the QLL typically describes the liquid-like interface between ice and air. For clarity, we will refer to the surface layer that forms at an air−ice interface as the quasi-liquid layer (QLL) and the remaining areas of possible solute enrichment (i.e., veins, nodes, grain boundaries, micropockets, etc.) as a liquid-like layer (LLL). It is unclear what role these liquid-like areas in snow/ice play in potential photochemical reactions and in altering the nature or rates of these reactions.

Several recent studies have described the physical nature of the QLL that occurs on the surface of snow/ice.[17,20,21] In terms of chemical reactions, studies discussing both qualitative and quantitative changes in reactivity upon freezing have been

* To whom correspondence should be addressed. Phone: 610-519-4881. Fax: 610-519-7167. E-mail: amanda.grannas@villanova.edu.

10.1021/jp073802q CCC: $37.00
Published on Web 10/06/2007

SCHEME 1: Photochemical Nucleophilic Substitution Reaction of Pyridine with *p*-Nitroanisole

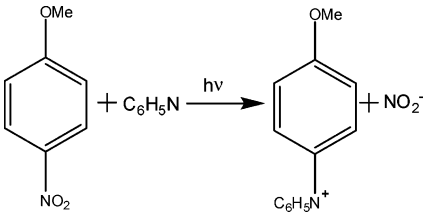

published.[22−25] However, relatively few studies are published that quantitatively probe organic photochemistry in frozen samples, with much of the published literature focusing on the chemistry of inorganic ions.[5,6,26−29] Studies investigating the photochemistry of organic compounds in ice are scant, and of those that are published, many focus on qualitative analysis to elucidate mechanisms and products of photochemistry, as opposed to quantitative understanding of reactivity differences between liquid and ice.[30−35]

Here, we discuss results from investigations of photochemical nucleophilic substitution reactions in liquid water, artificial snow, and ice. These findings provide further insight regarding the partitioning of organic solutes to the LLL and the impact this has on photochemical reactions of organic species. We use the reaction of *p*-nitroanisole with pyridine (a common chemical actinometer,[36] Scheme 1) to probe the changes in reactivity upon freezing and to study variables of environmental importance (temperature, solute concentration, freezing rate) that affect the nature of the LLL. Implications for atmospheric processes are discussed.

Experimental Methods

Solutions containing 3.3×10^{-3} M pyridine and 7.9×10^{-6} M *p*-nitroanisole were prepared in ultrapure water (18 MΩ· cm, Millipore Direct-Q) with pyridine (ReagentPlus) and a solution of *p*-nitroanisole (Aldrich, 97%) in acetonitrile (ACS reagent grade, Aldrich). All reagents and solvents were used without further purification. Solutions were placed in clear, borosilicate glass tubes (15 mm × 125 mm) with foil-lined caps. For liquid experiments, tubes were filled to the top to minimize headspace. For frozen samples, the tubes were not completely filled to allow for expansion upon freezing. Control experiments confirmed that the small amount of headspace present in the tubes did not affect measured concentrations of analytes within the condensed phase, as there was no loss of analyte to the headspace.

Three freezing methods were investigated. In one case, vials were filled with the liquid solution and placed in a temperature-controlled bath at room temperature, which was then allowed to cool to the temperature of the experiment using a Neslab CC100 immersion chiller at a rate of approximately 10 K/hour (freeze method 1). In the second case, vials were filled with the liquid solution and placed in a temperature-controlled freezer set to the desired temperature of the experiment (freeze method 2). In the third case, samples were submerged in liquid nitrogen and then placed in the temperature-controlled bath and allowed to warm to the temperature of the experiment, prior to irradiation (freeze method 3). Unless otherwise noted, data shown for ice samples were obtained using freeze method 1. Artificial snow samples were made using the method of Grannas et al.[10] In brief, a prepared solution was sprayed through a small-orifice nozzle into a dewar of liquid nitrogen. Ices were then collected and ground using a mortar and pestle to generate small, more-uniform pellets, about 0.25 mm in diameter (snow). Snow was

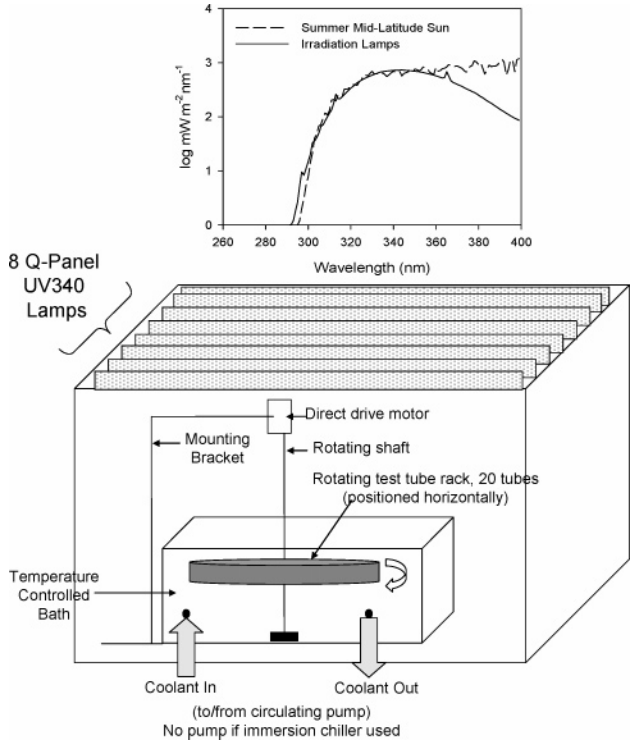

Figure 1. Top: Comparison of irradiation lamp output with natural sunlight (data provided by lamp manufacturer). Bottom: Schematic of irradiation apparatus.

then placed in (cold) borosilicate tubes and allowed to equilibrate overnight in a temperature-controlled freezer. Snow samples were irradiated following freeze method 2.

Temperature-controlled irradiation experiments were carried out using a custom-built irradiation apparatus fitted with Q-Panel (UV-340) lamps (Figure 1). These lamps reproduce reasonably well the UV radiation profile of natural mid-latitude noontime summer sunlight, as illustrated in Figure 1. Figure 1 represents the lamp emission; therefore, it is expected that some light scattering will occur off of the surface of the vials. However, because all samples were irradiated in the same type and size of vials and we are interested mainly in the comparison between experiments conducted under different phase and temperature conditions, this should have little impact on the interpretation of the results presented here. Samples were submerged in a temperature-controlled bath (either ethanol or an ethylene glycol/water mix, both of which are UV transparent), and the bulk sample was irradiated from the overhead lamps for a measured period of time. Bath temperatures between 268 and 273 K were controlled using a NesLab RTE-111 circulating chiller and an ethylene glycol/water bath, while temperatures lower than 268 K were controlled using a Neslab CC100 immersion chiller and an ethanol bath. Replicate experiments at several temperatures were performed using both baths, and it was found that the slight differences in bath geometry and bath liquid had no significant effect on measured PNA degradation rates.

Following irradiation, the frozen (ice or snow) samples were removed from the bath and placed into a beaker filled with cool water and covered in aluminum foil. Then, after approximately 5 min, the vials were placed into a beaker filled with warm water, also covered in aluminum foil. This sequence was done to prevent the vials from cracking upon warming; the aluminum foil was used to prevent any subsequent exposure to light. Once the samples had melted, the vials were hand-shaken, and 1 mL aliquots were placed into autosampler vials and sealed for immediate chromatographic analysis. Degradation of *p*-nitroani-

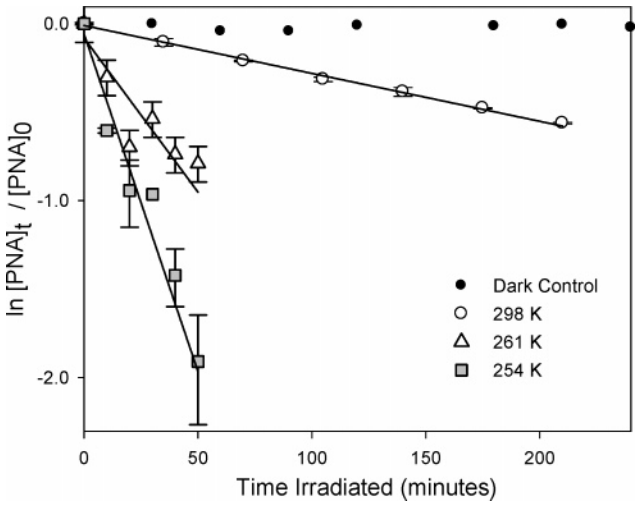

Figure 2. *p*-Nitroanisole photochemical degradation in liquid and ice samples at various temperatures. Samples kept dark (filled circles) showed no measurable *p*-nitroanisole degradation. The half-life (±1 s) of *p*-nitroanisole was calculated from individual degradation curves from experiments conducted in triplicate. Errors reported represent 1 standard deviation of the calculated half-life from three replicate, simultaneous experiments: 250 ± 12 min in liquid at 298 K (open circles), 40 ± 4 minutes in ice at 261 K (open triangles), and 18 ± 2 minutes in ice at 254 K (gray squares).

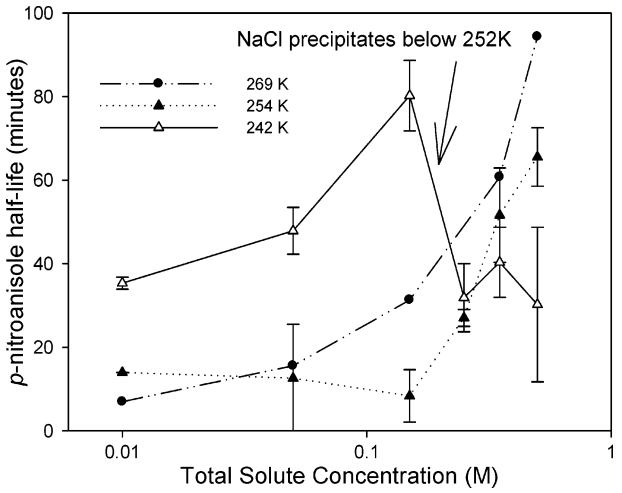

Figure 3. Measured half-life of *p*-nitroanisole as a function of total solute concentration (mol/L) at 269 (filled circles), 254 (filled triangles), and 242 K (open triangles). Lines are included merely as a visual guide and are not meant to represent quantitative trends.

sole was quantified via HPLC with UV−vis detection. Separation was achieved using a Fluophase PFP (ThermoElectron) column with guard column. The water/acetonitrile mobile phase composition was 50/50%, and the method was run isocratically with a mobile phase flow rate of 2 mL min^{-1}. The total run time was 5 min, with *p*-nitroanisole eluting around 2.2 min, monitored at a wavelength of 300 nm. Calibration involved analysis of *p*-nitroanisole standards in acetonitrile (range 1×10^{-6} to 8×10^{-6} M). The calibration curve for 10 μL injections resulted in a sensitivity of 2.25×10^9 area counts per M injected and $r^2 = 1.0$.

Results and Discussion

The degradation of *p*-nitroanisole (PNA) in liquid and ice at several temperatures is shown in Figure 2. The liquid experiment was conducted in the chiller apparatus with the bath liquid at room temperature. Dark controls were conducted using both liquid and frozen solutions at a number of temperatures, and no degradation was observed under any conditions. Additionally, dissolved oxygen had no effect on the chemistry, as the observed PNA half-life in an oxygen-purged solution was statistically indistinguishable from a solution made with oxygenated water.

Freezing of the solution, followed by irradiation, caused a sharp decrease in the observed half-life of PNA (from 250 min at 298 K to 18 min at 254 K), which we attribute to a freeze-concentration effect. As liquid water freezes, solutes can be excluded from the ice phase into the QLL, grain boundaries, veins, or nodes, increasing their apparent aqueous concentration, known as the freeze-concentration effect. This will affect the PNA/pyridine reaction due to a change in the actinometer quantum yield that is dependent on pyridine concentration (where $\Phi = 0.44$*[pyridine (mol/L)] + 0.00028), as discussed in Dulin and Mill[36]). It should be noted that reactions in frozen matrices might also be influenced by electric potential differences between ice and solution,[37−40] and ice itself could act as a catalytic surface.[41−43]

We investigated the role of ice as a catalytic surface by irradiating a liquid solution at 273 K both with and without added ice pellets (making up 15−25% of the solution mass) made from Milli-Q water. Solutions were made containing the typical pyridine and PNA concentrations and were then cooled to 273 K. Separately, ice pellets were generated in the same manner as artificial snow using Milli-Q water (containing no analytes). A known quantity (by mass) of ice was added to the cooled solutions, and then, the entire liquid + ice sample was irradiated for a given period of time between 272 and 273 K in the chilled bath. This method generally led to very little melting of the added ice (as assumed by visual inspection) during the course of the ~40 min experiment. After given irradiation times, the samples were removed from the irradiation apparatus, covered in foil, and allowed to melt completely. An aliquot of this solution (containing original liquid actinometer solution plus the melted ice) was analyzed to quantify PNA degradation in the liquid solution. Because the original volume of liquid solution was known, as well as the mass of added ice, the dilution effect caused by melting the ice after the irradiation was completed could be accounted for. Had there been a catalytic effect due to the ice surface, one would expect the PNA degradation rate to be faster in the samples with added ice pellets. However, we found that the PNA degradation rates were statistically indistinguishable between liquid samples with added ice and those without.

The effects of electric potential differences that may exist were also examined. As water freezes, anions and cations can become distributed unevenly between ice and solution, leading to a "freezing potential".[37−40] H_3O^+ or OH^- then migrates to neutralize the potential, leading to a highly variable pH in the liquid layer. PNA degradation was determined in ices of 0.50 M ionic strength containing either NaCl (negative freezing potential) or Na_2SO_4 (positive freezing potential) at 261 K. Comparison of the observed PNA degradation rates in NaCl- and Na_2SO_4-containing ices showed that they were not significantly different (70 ± 8 min with NaCl and 73 ± 1 min with Na_2SO_4). Therefore, changes in freezing potential did not alter the degradation of PNA under these conditions.

The correlation between total solute concentration and PNA half-life (at several temperatures) is illustrated in Figure 3. It is known that solute concentration significantly impacts the liquid content of ices,[17] with higher solute concentrations leading to a larger LLL. The solute concentration was increased by the addition of NaCl (at 0.01, 0.05, 0.15, 0.25, 0.35, and 0.50 M).

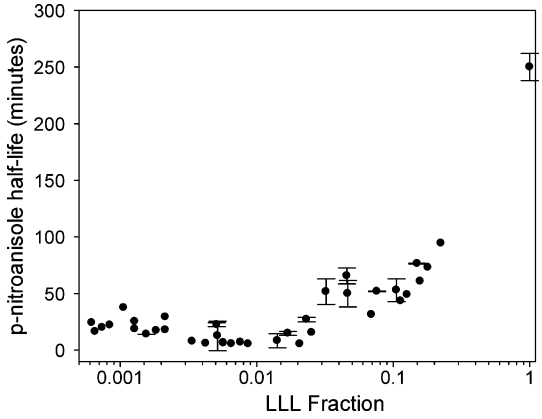

Figure 4. Measured half-life of *p*-nitroanisole as a function of the calculated liquid-like layer fraction. Error bars represent 1 standard deviation of the calculated half-life from replicate (typically three) experiments.

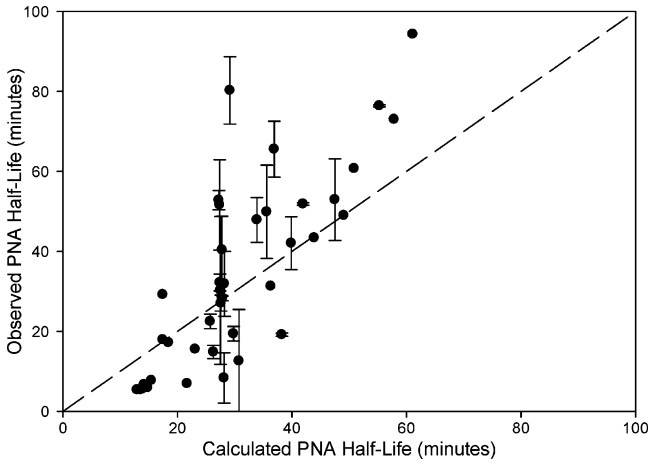

Figure 5. Comparison of the calculated and measured half-life of *p*-nitroanisole. The line shows 1:1 correlation.

The concentrations shown in Figure 3 include the presence of NaCl, PNA, pyridine, and acetonitrile. From Figure 3, there appear to be general trends of increased PNA half-life with solute concentration, but the behavior at various temperatures is seemingly irregular. It is necessary to include the combined effects of ionic strength, the presence of other solutes, and temperature on the LLL thickness in order to accurately describe the behavior of PNA photodegradation in this particular reaction system. The fraction of water molecules present as a LLL can be calculated as a function of solute concentration and temperature. This liquid-like fraction (ϕ) is calculated by eq 1[17]

$$\phi(T) \approx \frac{\bar{m}_{H_2O} R T_f}{1000 \Delta H_f^0} \left(\frac{T}{T - T_f}\right) C_T^0 \qquad (1)$$

where ϕ represents the fraction of H_2O molecules present in the "liquid-like layer" (or what we term the liquid-like layer (LLL) fraction), m_{H_2O} is the molecular weight of water, R is the ideal gas constant, T_f is the freezing temperature of pure water, T is the experimental temperature, ΔH_f is the melting enthalpy of water, and C_T is the total molal concentration of solutes in the completely unfrozen solution. Here, solutes include NaCl (if added), pyridine, PNA, and acetonitrile. Using this approach, both temperature and solute concentration can be accounted for in a calculation of the LLL fraction.

The correlation of the LLL fraction to the observed half-life for experiments conducted in ice is shown in Figure 4. It should be pointed out that experiments containing added NaCl at temperatures below the eutectic point (252 K) are not included here, as will be discussed later. The observed PNA half-life decreases substantially after freezing, down to LLL fractions of about 0.014. At smaller LLL fractions (from 6×10^{-5} to 0.013), the half-life levels off, with an average half-life of 16 ± 9 min. The behavior of PNA in ice can be compared to the known liquid-phase reactivity by assuming all solutes are excluded to the LLL upon freezing, thus leading to a substantial freeze-concentration effect that will subsequently impact the measured PNA half-life. Although the concentration dependence for this reaction has been previously studied (in liquid water),[36] the concentrations of pyridine used to establish the quantum yield dependence on [pyridine] did not exceed 0.0124 M. Assuming that all solutes are excluded to the LLL, the calculated concentration of pyridine in the LLL can reach 2 M in some experiments. It was thus necessary to establish the photochemical behavior of PNA in liquid water under very high pyridine concentrations. Liquid experiments were conducted with pyridine concentrations between 0.0033 and 3.0 M, and it was found that at pyridine concentrations greater than 0.07 M, the quantum yield relationship established by Dulin and Mill[36] no longer holds. The quantum yield reaches a maximum at [pyridine] = 0.11 M ($\Phi = 0.033$) and then decreases at higher concentrations (to $\Phi = 0.018$ at [pyridine] = 3.0 M). This is most likely due to interfilter effects from the high pyridine concentration. Additionally, several experiments involved addition of NaCl, used to modify the LLL fraction upon freezing. The liquid-phase reactivity of PNA is impacted by an ionic strength effect, where PNA reactivity slows (quantum yield decreases) at [NaCl] > 3 M. Taking the [pyridine] and ionic strength effects into account, it is still possible to calculate the expected half-life of the reaction, given the expected concentration of pyridine in the LLL. Assuming that all of the solutes partition into the LLL, it is possible to calculate the apparent concentration of pyridine in the LLL. This in turn is used, with the concentration-dependent quantum yield relationship (originally established by Dulin and Mill[36] and corrected for the nonlinearity at [pyridine] > 0.07 M and [NaCl] > 3 M), to calculate the expected PNA half-life in ice. Figure 5 and Table 1 illustrate the correlation between the calculated half-life and the observed half-life in ice samples. A linear regression of the data with a slope of 1 (shown by the dotted line in Figure 5) would indicate that the calculated and observed half-lives are in absolute agreement, that all pyridine is, in fact, excluded to a LLL where the chemistry is occurring, and that the established liquid-phase reactivity can be extrapolated to ice conditions based solely on the concentration enhancement effect. Of the 38 separate experiments shown in Figure 5, the calculated and observed PNA half-life agrees within experimental variability for 13 experiments (34% of the experiments). The discrepancy between calculated and observed PNA half-lives becomes significantly greater and much more variable as the LLL becomes smaller, as illustrated in Figure 6. An important factor to consider is the actual nature of the LLL. The calculations performed above assume that all solutes partition to the LLL, that an equilibrium exists between the ice and LLL, and that the reaction can still be described by liquid-phase kinetics. The fundamental properties of the various "phases" present in snow/ice, however, are still under debate, as discussed in a recent review by Dominé et al.[19] Does the LLL present in ice exist as supercooled water or a disordered phase? Can liquid-phase kinetics adequately describe reactivity in the LLL of ice? The results presented here indicate that either the assumption that all solutes partition to

TABLE 1: Comparison of the Calculated PNA Half-Live as a Function of Liquid Content of the Sample for Representative Samples Spanning the Range of LLL Fractions Observed; the Calculated Half-Lives have been Corrected for the Nonlinearity of the Relationship of Quantum Yield to LLL [pyridine] at Concentrations > 0.07 M and for the Effect of Ionic Strength at LLL [NaCl] > 3 M

experimental conditions (reported concentrations refer to the unfrozen solution)	LLL fraction (eq 1)	calculated [pyr] in LLL (M)	$t_{1/2}$ calc (min)	$t_{1/2}$ obs (min)	% error (obs − calc)/obs*100
ice, 269K, 0.5 M NaCl	0.224	0.0148	61	94.3	35
ice, 268 K, 0.5 M NaCl	0.180	0.0184	58	73	21
ice, 269 K, 0.35 M NaCl	0.158	0.0210	51	61	16
ice, 267 K, 0.5 M NaCl	0.150	0.0221	55	76	27
ice, 268 K, 0.35 M NaCl	0.127	0.0262	49	49	0
ice, 269 K, 0.25 M NaCl	0.113	0.0292	44	44	0
ice, 267 K, 0.35 M NaCl	0.106	0.0314	48	53	10
ice, 267 K, 0.25 M NaCl	0.076	0.0436	42	52	19
ice, 269 K, 0.15 M NaCl	0.059	0.0564	40	42	5
ice, 269 K, 0.05 M NaCl	0.025	0.131	23	16	−49
ice, 254 K, 0.25 M NaCl	0.023	0.143	28	27	−2
ice, 242 K, 0.25 M NaCl	0.014	0.243	28	32	11
ice, 272.4 K	0.00866	0.382	13	6	−126
ice, 269 K, 0.01 M NaCl	0.00761	0.435	22	7	−213
ice, 271.1 K	0.00653	0.507	14	6	−133
ice, 270.8 K	0.00569	0.582	14	7	−111
ice, 254 K, 0.05 M NaCl	0.00512	0.641	31	13	−144
ice, 270 K	0.00423	0.782	15	6	−151
ice, 269.2 K	0.00337	0.983	15	8	−101
ice, 254 K, 0.01 M	0.00156	2.12	42	14	−203
ice, 254 K	0.000655	5.05	37	16	−126

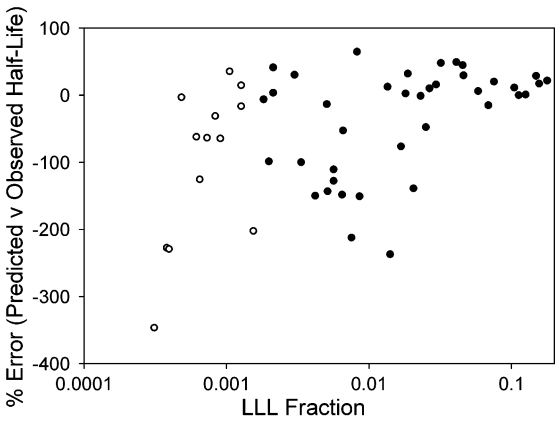

Figure 6. Error in the PNA half-life prediction as a function of the LLL fraction. Negative errors indicate that the predicted half-life is longer than what is observed experimentally. Open circles represent experiments where the calculated concentration of PNA in the LLL exceeded its liquid water solubility.

the LLL is not valid (which subsequently leads to an invalid calculation of the LLL fraction in a given sample) or that liquid-phase kinetics cannot be applied to this reaction occurring in the ice phase, particularly under conditions where the LLL is presumed to be the smallest. A number of published studies have shown, for example, that nitrate photolysis in ice and snow can, in fact, be described by liquid-phase kinetics.[5,28,44−46] The authors found good agreement between the experimental results and a description of the reactivity using the known liquid-phase mechanism and kinetics. It could be expected that, since ionic species are much more soluble in liquid water than in ice, one would observe ionic concentrations to be much higher in the LLL than those in the solid, and a complete partitioning to the LLL might be reasonable (but, as Dominé et al.[19] point out, convincing evidence of this is still lacking, at present). The behavior of many neutral organic species, however, is complicated by lower liquid water solubility and the relative hydrophobic/hydrophilic properties of different species. Preferential partitioning of molecules between solid ice and the LLL should be expected based on solubility alone, which would invariably affect observed reactivity of bimolecular reactions occurring in a liquid-like layer. Because the solubility of pyridine (completely miscible with water) is much greater than that of PNA (<0.006 mol/L), it will preferentially be excluded to the LLL, whereas PNA might form solid solutions, precipitate at the ice/liquid interface, or be trapped within the bulk ice structure. Hence, a bimolecular reactivity "limit" might be expected at very low LLL fractions (and could explain the leveling off of PNA half-life as the LLL fraction decreased). Several experiments conducted here resulted in a calculated PNA concentration (in the LLL) that exceeded the solubility of PNA (open circles shown in Figure 6). In many cases, these led to the largest deviation between observed and predicted PNA half-life.

Arguably, the experiments discussed here contain solute concentrations well above those which are typically observed in environmental snow/ice. However, the presumed LLL content of environmental samples is likely very small, thus leading to a large enrichment factor. For example, Voss et al.[21] calculated QLL fractions for environmental snowpack and ice aerosols ranging from $>10^{-3}$ to $<10^{-5}$. An organic solute present in a snow sample at 1 μM (i.e., the concentration in the total melted sample) that is subject to partitioning into a LLL fraction of 10^{-5} would experience an enrichment factor of 10,000, resulting in a LLL concentration of 0.1 M. If this theoretical organic species were PNA, this would far exceed its expected solubility. On the other hand, a calculation such as this assumes that the same solubility limits apply in the LLL as those in pure liquid water, an arguably tentative assumption. Thus, it is imperative to understand the fundamental nature of the various liquid-like regimes that may exist in snow/ice and also the physical properties solutes exhibit in these quasi-liquids.

Below the eutectic point (252 K), NaCl present in the sample precipitates from solution, leading to a significant decrease in the LLL fraction, as illustrated by the NMR results of Cho et al.[17] Their results showed that at low [NaCl] (0.010 M), a

significant fraction of ions remains in the liquid state to as low as 228 K; however, at higher [NaCl] (0.50 M), over 99% of NaCl precipitates as $NaCl*2H_2O$, leading to a simultaneous drop in the LLL fraction. Our results confirm the importance of this process to concentration-dependent photochemical reactions occurring in the LLL. As illustrated in Figure 3, the PNA half-life measured at 242 K increases from 0 to 0.15 M NaCl (as expected, given an increasing LLL size) but then drops significantly at ionic strengths between 0.25 and 0.50 M, indicating a shrinkage of the LLL and a subsequent increased concentration of reactants. Cho et al.[17] attribute this behavior to a kinetic effect of competing rates of diffusion of ions prior to precipitation versus solidification of the pure ice phase. In fact, the LLL fraction measured by Cho et al.[17] for 0.50 M NaCl is smaller than that at 0.010 M, at temperatures below the eutectic point. In comparison, the PNA half-life measured in our experiments at 242 K (below the eutectic point) at solute concentrations above 0.25 M is similar to the half-life measured at 0.010 M, within the variability of the experimental data. From the measured PNA half-lives, it could be inferred that NaCl precipitation does not become significant (and thus, the LLL does not shrink significantly) until [NaCl] of greater than 0.15 M. Because Cho et al.[17] do not report experimental NMR data for ionic strengths between 0.010 and 0.50 M, we cannot directly compare our measured half-lives to their results at intermediate ionic strengths, but the relationship between PNA photodegradation and LLL size follows the general trend that they discuss.

Samples (with no added salts) were frozen using three methods to examine the impact of freezing method and rate, as described in the experimental methods section. Comparison of PNA degradation rates at 263 K showed no statistically significant difference among the three freezing methods used to generate ice samples. The distribution of PNA between the liquid and ice was investigated experimentally by freezing a liquid solution from the bottom to the top of the borosilicate tubes. This was done by slowly immersing the vial in either liquid nitrogen (for a fast freeze) or in chilled ethanol at 258 K (for a slow freeze). Once certain fractions of the sample froze, all of the remaining supernatant liquid was removed. PNA was quantified in the supernatant liquid and melted ice layers to determine the amount of PNA "enrichment" in the liquid layer compared to that in the bulk ice. In both cases (fast freeze and slow freeze), a slight enrichment of PNA was observed in the supernatant liquid (about 10%). However, because the freezing rate is relatively fast, freezing was not occurring under equilibrium conditions, and it is likely that PNA was segregated to, for example, grain boundaries, veins, and nodes present in the polycrystalline ice layer or in micropockets of PNA that may have existed within the bottom ice, which could not be physically separated from the bulk ice using the methods described here. Thus, a significant concentration enhancement is not observed experimentally in a bulk experiment such as this. Because it is unlikely that we achieved equilibrium conditions, we may not necessarily expect to see a large difference in the photochemical degradation rates due to these three different (arguably nonequilibrium) freezing methods. More specifically, the comparisons ideally should be made between samples containing identical analyte concentrations and frozen slowly to achieve equilibrium conditions and frozen under nonequilibrium conditions to establish a possible significant difference between the solute partitioning and, thus, photochemical degradation rates.

TABLE 2: Comparison of Measured *p*-Nitroanisole Half-Lives Measured in Snow and Ice Samples; Standard Deviations are Obtained from Results of Replicate Experiments

temperature (K)	sample type	ionic strength ([NaCl] in unfrozen solution, M)	measured *p*-nitroanisole half-life (min)	standard deviation (1s)
258	ice	0.05	9	3
258	snow	0.05	19	2
258	ice	0.15	14.3	0.9
258	snow	0.15	28.2	0.6
258	ice	0.25	18.0	0.4
258	snow	0.25	32	2
269	ice	0	8	n/a
269	snow	0	12	2

The photochemical degradation of PNA was compared in snow and ice samples at several temperatures and ionic strengths. Table 2 summarizes the results obtained. In all cases, the degradation of PNA was slower in snow samples (when compared to ice samples irradiated under the same conditions of temperature and solute concentration). This longer half-life could result from increased scattering of incident radiation from the snow crystal surfaces, leading to an overall smaller photon flux throughout the snow sample depth of approximately 15 mm.

The results obtained here indicate that the photochemical reactivity of pollutants in snow and ice is significantly impacted by the freeze-concentration effect. This will be most important for bimolecular reactions, as these results indicate that the primary influence on reaction rate is reactant concentration, rather than any surface catalysis or freezing potential effects. How freezing may affect direct photochemical processes (i.e., where absorption of photons leads directly to product formation) is less clear and requires further experimentation. It should be pointed out that these experiments were completed at relatively high concentrations, compared to what would be observed in natural environmental samples where organic carbon concentrations are in the ppb−ppm range (μg C L^{-1} to mg C L^{-1}) and where ionic strengths are also relatively low (μM−mM). The partitioning behavior is also likely to be related to the concentration and water solubility of the molecule and should be a subject of further experimentation.

As shown in these results, the reaction rates of this particular bimolecular reaction in ice can, in some cases, be described using liquid rate coefficients but are significantly faster in ice due to increased reactant concentrations. More importantly, at small LLL fractions, the comparison of ice and liquid reactivity is no longer valid, either due to invalid assumptions made regarding solute partitioning or because the reactions are not occurring in a phase where liquid-phase kinetics can be applied. Future investigations will need to establish the exact location of the solutes under various conditions, including temperature, solute concentration, and freezing methods (including both equilibrium and nonequilibrium freezing). This is a challenging experimental proposition but one that must be addressed so that correlations between laboratory experiments and field observations can be made.

The photochemical generation of reactive oxygen species (e.g., OH, $^1O_2$, O_2^-) and subsequent reaction with organic materials present in natural snowpacks has been hypothesized to be a source of low-molecular-weight species that can then be emitted to the atmosphere.[8,10,27,47] The results presented here indicate that the rate of these reactions will be highly dependent on snow and ice properties, particularly temperature and solute

content. A simple extrapolation of liquid-phase mechanisms and kinetics may not be a valid method to predict the reactivity of organic species in snow and ice. It is necessary to have a fundamental understanding of the liquid content of a given sample as well as the likelihood of preferential partitioning of the reactants into the liquid or liquid-like phase, which will ultimately depend on the nature of the ice/snow, reactant concentration, and aqueous solubility of the reactant(s).

Acknowledgment. This work was financed, in part, by NSF Grant ATM-0547435. We thank P. B. Shepson and F. Dominé for helpful discussion, as well as the comments of two anonymous reviewers, which greatly improved the quality of the manuscript.

References and Notes

(1) Foster, K. L.; Plastridge, R. A.; Bottenheim, J. W.; Shepson, P. B.; Finlayson-Pitts, B. J.; Spicer, C. W. *Science* **2001**, *291*, 471.

(2) Barrie, L. A.; Bottenheim, J. W.; Schnell, R. C.; Crutzen, P. J.; Rasmussen, R. A. *Nature* **1988**, *334*, 138.

(3) Lu, J. Y.; Schroeder, W. H.; Barrie, L. A.; Steffen, A.; Welch, H. E.; Martin, K.; Lockhart, L.; Hunt, R. V.; Boila, G.; Richter, A. *Geophys. Res. Lett.* **2001**, *28*, 3219.

(4) Honrath, R. E.; Peterson, M. C.; Guo, S.; Dibb, J. E.; Shepson, P. B.; Campbell, B. *Geophys. Res. Lett.* **1999**, *26*, 695.

(5) Chu, L.; Anastasio, C. *J. Phys. Chem. A.* **2003**, *107*, 9594.

(6) Boxe, C. S.; Colussi, A. J.; Hoffmann, M. R.; Murphy, J. G.; Wooldridge, P. J.; Bertram, T. H.; Cohen, R. C. *J. Phys. Chem. A.* **2005**, *109*, 8520.

(7) Stemmler, K.; Ammann, M.; Donders, C.; Kleffmann, J.; George, C. *Nature* **2006**, *440*, 195.

(8) Sumner, A. L.; Shepson, P. B. *Nature* **1999**, *398*, 230.

(9) Guimbaud, C.; Grannas, A. M.; Shepson, P. B.; Fuentes, J. D.; Boudries, H.; Bottenheim, J. W.; Dominé, F.; Houdier, S.; Perrier, S.; Biesenthal, T. B.; Splawn, B. G. *Atmos. Environ.* **2002**, *36*, 2743.

(10) Grannas, A. M.; Shepson, P. B.; Filley, T. R. *Global Biogeochem. Cycles* **2004**, *18*, doi:10.1029/2003GB002133.

(11) Swanson, A. L.; Blake, N. J.; Dibb, J. E.; Albert, M. R.; Blake, D. R.; Rowland, F. S. *Atmos. Environ.* **2002**, *36*, 2671.

(12) Boudries, H.; Bottenheim, J. W.; Guimbaud, C.; Grannas, A. M.; Shepson, P. B.; Houdier, S.; Perrier, S.; Dominé, F. *Atmos. Environ.* **2002**, *36*, 2573.

(13) Michalowski, B. A.; Francisco, J. S.; Li, S. M.; Barrie, L. A.; Bottenheim, J. W.; Shepson, P. B. *J. Geophys. Res.* **2000**, *105*, 15131.

(14) Grannas, A. M.; Shepson, P. B.; Guimbaud, C.; Dominé, F.; Albert, M.; Simpson, W.; Bottenheim, J. W.; Boudries, H. *Atmos. Environ.* **2002**, *36*, 2733.

(15) Faraday, M. *Philos. Mag.* **1859**, *17*, 162.

(16) Wei, X.; Miranda, P. B.; Shen, Y. R. *Phys. Rev. Lett.* **2001**, *86*, 1554.

(17) Cho, H.; Shepson, P. B.; Barrie, L. A.; Cowin, J. P.; Zaveri, R. *J. Phys. Chem. B* **2002**, *106*, 11226.

(18) Koop, T.; Kapilashrami, A.; Molina, L. T.; Molina, M. J. *J. Geophys. Res.* **2000**, *105*, 26393.

(19) Dominé, F.; Albert, M.; Huthwelker, T.; Jacobi, H.-W.; Kokhanovsky, A. A.; Lehning, M.; Picard, G.; Simpson, W. R. *Atmos. Chem. Phys. Discuss.* **2007**, *7*, 5941.

(20) Döppenschmidt, A.; Butt, H. J. *Langmuir* **2002**, *16*, 6709.

(21) Voss, L. F.; Henson, B. F.; Wilson, K. R.; Robinson, J. M. *Geophys. Res. Lett.* **2005**, *32*, doi:10.1029/2004GL022010.

(22) Bruice, T. C.; Butler, A. R. *J. Am. Chem. Soc.* **1964**, *86*, 4104.

(23) Alburn, H. E.; Grant, N. H. *J. Am. Chem. Soc.* **1965**, *87*, 4174.

(24) Takenaka, N.; Ueda, A.; Daimon, T.; Bandow, H.; Dohmaru, T.; Maeda, Y. *J. Phys. Chem.* **1996**, *100*, 13874.

(25) Takenaka, N.; Daimon, T.; Ueda, A.; Sato, K.; Kitano, M.; Bandow, H.; Maeda, Y. *J. Atmos. Chem.* **1998**, *29*, 135.

(26) Chu, L.; Anastasio, C. *J. Phys. Chem. A* **2005**, *109*, 6264.

(27) Anastasio, C.; Jordan, A. L. *Atmos. Environ.* **2004**, *38*, 1153.

(28) Dubowski, Y.; Colussi, A. J.; Hoffmann, M. R. *J. Phys. Chem. A* **2001**, *105*, 4928.

(29) Dubowski, Y.; Colussi, A. J.; Boxe, C.; Hoffmann, M. R. *J. Phys. Chem. A* **2002**, *106*, 6967.

(30) Dubowski, Y.; Hoffmann, M. R. *Geophys. Res. Lett.* **2000**, *27*, 3321.

(31) Klán, P.; Del Favero, D.; Ansorgova, A.; Klánová, J.; Holoubek, I. *Environ. Sci. Pollut. Res.* **2001**, *8*, 195.

(32) Klánová, J.; Klán, P.; Nosek, J.; Holoubek, I. *Environ. Sci. Technol.* **2003**, *37*, 1568.

(33) Blaha, L.; Klanova, J.; Klan, P.; Janosek, J.; Skarek, M.; Ruzicka, R. *Environ. Sci. Technol.* **2004**, *38*, 2873.

(34) Matykiewiczova, N.; Kurkova, R.; Klánová, J.; Klán, P. *J. Photochem. Photobiol., A* **2007**, *187*, 24.

(35) Guzman, M. I.; Colussi, A. J.; Hoffmann, M. R. *J. Phys. Chem. A* **2006**, *110*, 3619.

(36) Dulin, D.; Mill, T. *Environ. Sci. Technol.* **1982**, *16*, 815.

(37) Workman, E. J.; Reynolds, S. E. *Phys. Rev.* **1950**, *78*, 254.

(38) Lodge, J. P., Jr.; Baker, M. L.; Pierrard, J. M. *J. Chem. Phys.* **1956**, *24*, 716.

(39) Gross, G. W.; Wong, P. M.; Humes, K. *J. Chem. Phys.* **1977**, *67*, 5264.

(40) Finnegan, W. G.; Pitter, R. L.; Young, L. G. *Atmos. Environ.* **1991**, *25A*, 2531.

(41) Liu, Z. F.; Siu, C. K.; Tse, J. S. *Chem. Phys. Lett.* **1999**, *309*, 335.

(42) Bolton, K.; Pettersson, J. B. *J. Am. Chem. Soc.* **2001**, *123*, 7360.

(43) Duvernay, F.; Chiavassa, T.; Borget, F.; Aycard, J.-P. *J. Am. Chem. Soc.* **2004**, *126*, 7772.

(44) Honrath, R. E.; Guo, S.; Peterson, M. C.; Dziobak, M. P.; Dibb, J. E.; Arsenault, M. A. *J. Geophys. Res.* **2000**, *105*, 24183.

(45) Cotter, E. S. N.; Jones, A. E.; Wolff, E. W.; Baugitte, S. J.-B. *J. Geophys. Res.* **2003**, *108*, 4147.

(46) Jacobi, H.-W.; Annor, T.; Quansah, E. *J. Photochem. Photobiol., A* **2006**, *185*, 371.

(47) Dibb, J. E.; Arsenault, M. *Atmos. Environ.* **2002**, *36*, 2513.